Inter-Carrier Interference Analysis for High Speed Trains based on Broadband Channel Measurements

Eric Simon*, Florian Kaltenberger†
*IEMN laboratory, University of Lille 1, France
†EURECOM, Sophia Antipolis, France

***Abstract*—This paper presents an analysis of inter-carrier interference (ICI) in high speed trains. The ICI is caused by the motion of the receiver together with the carrier frequency offset (CFO). It results in a degradation of the reliability of the OFDM transmission. The analysis is based on a channel sounding measurement campaign for cellular broadband wireless communications with high speed trains that was carried out in the context of CORRIDOR project. The considered scenario corresponds to a railway deployed network, where the base station is located directly next to the railway line. We present the ICI power obtained with the measurement campaign and some theoretical results for a simple channel model that captures the main effects observed in the measurements.**

***Index Terms*—ICI, Channel Sounding, High-speed train**

I. Introduction

This paper is based on the results of a channel sounding measurement campaign for cellular broadband wireless communications with high speed trains that was carried out in the context of CORRIDOR project [1]. The sounding signal is an OFDM signal, whose parameters are similar to those of the LTE standard. When the channel is time-invariant, the signal transmitted on a given subcarrier does not interfere with adjacent subcarriers thanks to the orthogonality between the subcarriers which is assured as long as the length of the cyclic prefix is greater than the channel order. Thus, the transmitted symbols can be easily retrieved by simply inverting the channel on each subcarrier. In a high mobility scenario, the resulting Doppler shift expands the signal bandwidth, destroying the orthogonality between subcarriers. Consequently, the signal transmitted on a given subcarrier is no longer concentrated on this subcarrier at the receiver but spreads out on the adjacent subcarriers. The higher the Doppler, the further away the signal is distributed from its original subcarrier. This phenomenon is called inter-carrier interference (ICI) [2]. Note that the carrier frequency offset (CFO) originating from a mismatch between the transmitter oscillator and receiver oscillator has the same effect on the signal than the Doppler shift and also yields ICI. If the ICI level is high, the classical simple receivers perform poorly. Indeed, since each subcarrier is contaminated by the signal from adjacent subcarriers, it is no longer possible to retrieve the transmitted signal by simply inverting the channel on each subcarrier. Consequently, more complex receivers have to be used to deal with this phenomenon [3], [4], [5], [6]. Thus, it is of importance to quantify the level of the ICI so as to adapt the receivers accordingly.

Sampling rate (Msps)	15.36
OFDM symbol duration	66 μs
Cyclic prefix length	16 μs
OFDM symbol size N	1024
Useful OFDM carriers N_c	600

TABLE I
Sounding signal parameters

In order to study the ICI, we have designed a specific sounding signal by nulling one subcarrier out of two. This way, the signal received on the null-subcarriers corresponds to the ICI, and thus can be measured. First, we present the results of the measured ICI power. Then, we consider a simple channel model and we theoretically calculate the ICI power. Finally, these theoretical results are compared with the measurements.

To the best of the author's knowledge, this is the first time that the power of the ICI is measured in high speed trains.

The rest of the paper is organized as follows. We first present the measurement equipment and scenarios in Section II. We present the results of the measurement for the ICI in Section III and the theoretical calculation of the ICI in Section IV. Finally we give conclusions in Section V.

II. Measurement Description

A. Sounding Signal

For our ICI analysis, we consider the band of 10 MHz around 2.605 GHz of the measurement campaign. The design uses four transmitting antennas and two receiving antennas. The transmitted signal is an OFDM signal, whose parameters are similar to those of the LTE standard. Table I summarizes the signal parameters.

The signal is framed to 10 ms, or 120 OFDM symbols. The first symbol of each frame contains the LTE primary synchronization sequence (PSS) and the rest of the signal is filled with OFDM modulated random QPSK symbols. Note that the empty subcarriers around the PSS will also be used for the noise variance estimation in the ICI analysis. In order to measure inter carrier interference (ICI) in high mobility scenarios, we only use every second subcarrier. To obtain individual channel estimates from the different transmitting antennas, we use an orthogonal pilot pattern as depicted in Figure 1, where A0, A1, A2, A3 mean signals from antennas 0, 1, 2, 3 respectively.

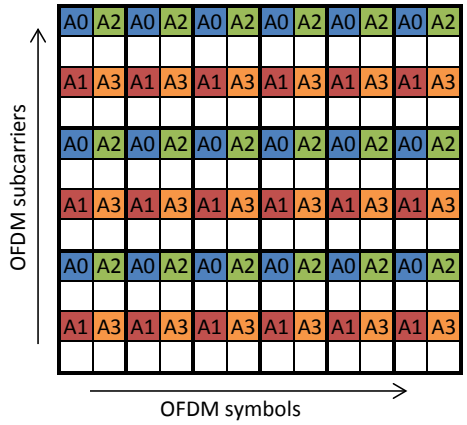

Fig. 1. Allocation of resource elements (RE) to antennas. Empty REs are unused to measure inter-carrier interference (ICI).

B. Measurement Equipment and Scenario

The equipment used for the measurement campaign is described in detail in [1]. The basis for both transmitter and receiver of the channel sounder is the Eurecom ExpressMIMO2 software defined radio card, which are part of the OpenAir-Interface platform[1]. At the base station (the transmitter) we have used two sectorized, dual polarized HUBER+SUHNER antennas with a 17dBi gain (ref SPA 2500/85/17/0/DS). At the train (the receiver) we used used two Sencity Rail Antennas from HUBER+SUHNER (ref SPA 2400/50/12/10/V) were mounted, which provide two ports with 11dBi gain each: one pointing to the front and one to the back of the train [7]. However, for the experiments we have only used one port from each antenna that are pointing in the same direction.

The measurements were carried on board of the IRIS320 train[2] along the railway line "LGV Atlantique" around 70 km southwest of Paris. The base station (eNB in LTE speak) is located right next to the railway line at a height of about 12m. The train passes the area with a speed of approximately 300 km/h. The receiver antennas are mounted on the top of the train, approximately half way between the front and the rear and there was always a line-of-sight between the base station and the terminal antenna. The two runs *Trial 2–Run 1* and *Trial 2–Run 3* of [1] are being investigated. The only difference between the two is that in *Trial 2–Run 1* half of the TX antennas pointing at one direction of the railway, and the other half are pointing at the opposite direction while in *Trial 2–Run 3* all the 4 TX antennas are oriented in the same direction.

C. Delay-Doppler Power Profile Analysis

Figures 2 and 3 show the Doppler delay power spectrum for Trial 2-Run 3 and Trial 2-Run 1 respectively. The method to obtain the Doppler delay spectrum is presented in detail in [1]. It can be seen that the total frequency shift combining

[1]http://www.openairinterface.org
[2]http://en.wikipedia.org/wiki/SNCF_TGV_Iris_320

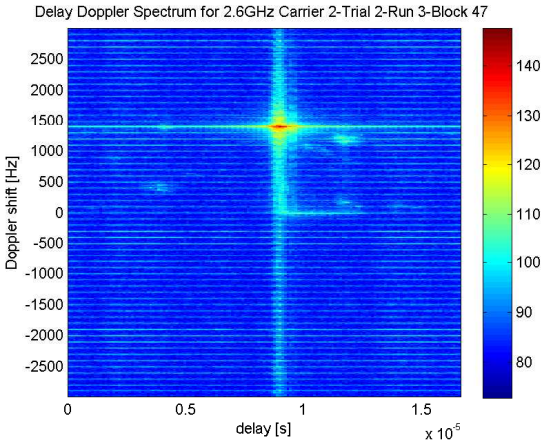

Fig. 2. Trial 2-Run 3. Delay Doppler Spectrum.

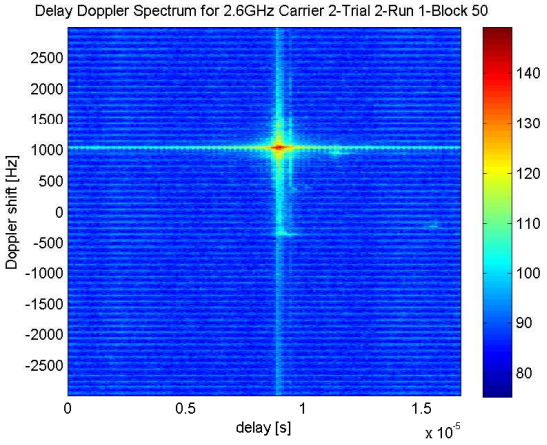

Fig. 3. Trial 2-Run 1. Delay Doppler Spectrum.

both CFO and Doppler is around 1390 Hz for Run 3 and 1050 Hz for Run 1.

It is worth noting that a real modem would be able to compensate the CFO online using the PSS and the pilot symbols. However, in our setup this was not possible since the terminal was storing only raw IQ samples and no real-time processing was possible. For the further discussion it is not important where the actual frequency shift of the measurements comes from; only the total frequency shift matters. Additionally, such high values of frequency shifts would be consistent with realistic values for higher carrier frequencies. For instance, 1050Hz would correspond to a speed of 324km/h at 3.5GHz.

III. Measured ICI Power

The objective of this section is to obtain the ICI power from the measurements. For the values of speed and CFO considered in the measurements, only the two adjacent subcarriers $n+1$ and $n-1$ receive a significant level of power from subcarrier n. The signal power spread on further subcarriers is negligible. Thus, to measure the level of ICI, we calculate the ratio of the signal power at the null-subcarriers to the signal power at the direct adjacent subcarriers.

To obtain the signal power at subcarrier n, we first have to estimate the noise power in order to subsequently remove it from the measurement. To do so, we use the LTE primary synchronization signal (PSS). The PSS is an OFDM symbol with signal on the 60 subcarriers at both ends, and nothing between them. So we use these null subcarriers to estimate the noise power, denoted P_{noise}. The noise power estimation is updated at each frame.

Let $y_{n,k}$ denote the received signal after the OFDM receiver, where $n = 0, \ldots, N_c - 1$ is the subcarrier index and k is the OFDM symbol index. $N_s = 120$ OFDM symbols make up one frame and 100 frames make up one block. First, we calculate the signal powers by averaging the subcarriers over a frame and removing P_{noise}. For antennas A0, A1, we obtain:

$$P^{01}_{n,i,j} = \frac{2}{N_s} \sum_{k=0}^{N_s/2-1} |y_{n,2k+N_s i+100N_s j}|^2 - P_{\text{noise}}, \quad (1)$$

and for antennas A2, A3:

$$P^{23}_{n,i,j} = \frac{2}{N_s} \sum_{k=0}^{N_s/2-1} |y_{n,2k+1+N_s i+100N_s j}|^2 - P_{\text{noise}}, \quad (2)$$

where i is the frame index and j the block index.

We calculate now the ratio of the signal power on the null-subcarriers, corresponding to the ICI power, to the mean signal powers on the adjacent subcarriers. These power ratios are averaged over blocks of 100 frames:

$$R^{01}_j = \frac{1}{100} \sum_{i=0}^{99} \frac{2}{N_c} \sum_{n=0}^{N_c/2-1} \frac{P^{01}_{2n+1,i,j}}{(P^{01}_{2n,i,j} + P^{01}_{2n+2,i,j})/2} \quad (3)$$

$$R^{23}_j = \frac{1}{100} \sum_{i=0}^{99} \frac{2}{N_c} \sum_{n=0}^{N_c/2-1} \frac{P^{23}_{2n+1,i,j}}{(P^{23}_{2n,i,j} + P^{23}_{2n+2,i,j})/2} \quad (4)$$

These power ratios express the relative ICI power and will be compared with the theory in the next section.

Fig. 4 shows the power ratios for Trial 2–Run 3. The scenario of this run clearly appears, with the four antennas pointing toward the train. It can be seen that the train passes the eNB around block 120. When the train is departing the eNB, the calculated power ratios have no meaning since there is no signal any more. It is observed that the power ratio has nearly the same value between blocks 30 and 120. This is understood since the ICI power value depends on the speed and CFO which do not vary over this observation window. On average, we find -15 dB.

Fig. 5 shows the power ratios for Trial 2–Run 1. This time antennas A0, A1 are pointing toward the approaching train, and A2, A3 in the opposite direction. The train passes the eNB around block 90. When the train is approaching the eNB, the average value of power ratio R^{01}_j is around -16 dB.

IV. Theoretical ICI power

The first interpretations from the measurement campaign distinguished two phases [1], the first one corresponds to the train approaching the eNB and the second one to the train leaving the eNB. It was shown that these phases have different propagation models. Since the calculation of the theoretical ICI power requires a channel model, one phase has to be selected. We focus on the first phase since it corresponds to the scenario of Trial 2-Run 3 for which the four antennas are pointing towards the approaching train, and also to the scenario of Trial 2-Run 1 for antennas A0, A1. For the approaching train phase, it was shown in [1] that the channel mainly consists of the line of sight (LOS). Note that when the train is departing from the eNB, the channel model is more complicated [1]. Let us first define the notations of the OFDM system model.

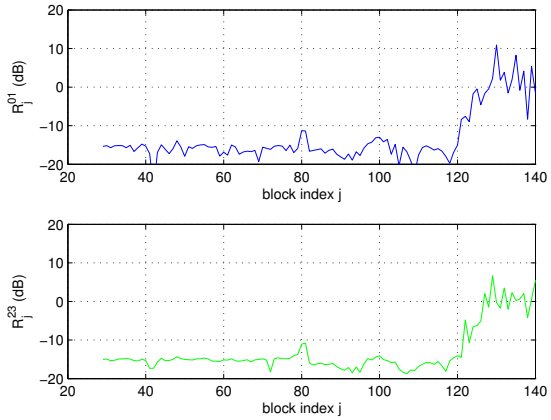

Fig. 4. Trial 2-Run 3. Power ratios (3), (4) as a function of the block index.

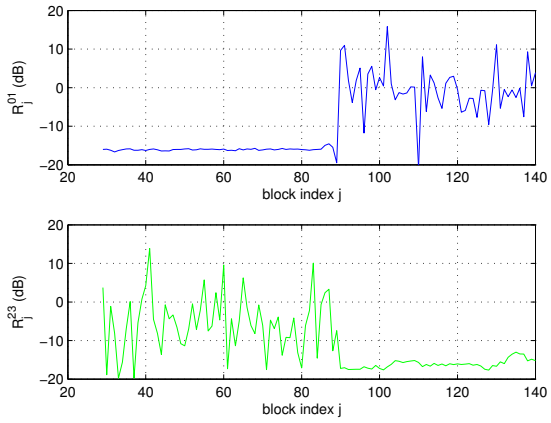

Fig. 5. Trial 2-Run 1. Power ratios (3), (4) as a function of the block index.

A. OFDM System Model

Let f_c be the carrier frequency and Δf the carrier frequency offset due to the mismatch between the transmitter and receiver oscillators. Let us consider an OFDM system with a symbol size N and a cyclic prefix length N_g. The duration of an OFDM symbol is $T_{\text{sym}} = (N + N_g)T_s$ where T_s is the sampling time. Let $s_{n,k}$, $n = 0, \ldots, N-1$ be the transmitted data symbol on the subcarrier $n - N/2$ of the kth OFDM symbol. The $\{s_{n,k}\}$ are QPSK pilot symbols normalized to

one. The time-varying channel impulse response is a single-path model where the CFO has been included to ease the calculations:

$$h(t,\tau) = \alpha_0(t)\delta(\tau - \tau_0)e^{j2\pi\Delta ft} \quad (5)$$

where $\alpha_0(t)$ is the complex amplitude of the LOS and τ_0 the corresponding physical time delay. We consider here a deterministic approach, *i.e.* $\alpha_0(t) = \rho_0 e^{-j2\pi f_c \tau_0(t)}$ with ρ_0 the modulus and $\tau_0(t) = \tau_0(0) + \frac{v_m cos(\theta_0)}{c}t$, where θ_0 is the angle of arrival of the ray l, v_m is the speed of the train and c is the speed of light. This yields $\alpha_0(t) = \rho_0 e^{-j2\pi f_c \tau_0(0)} e^{-j2\pi f_D cos(\theta_0)t}$, where $f_D = \frac{f_c v_m}{c}$ is the maximum Doppler frequency. Note that τ_0 can be safely assumed to be constant in $\delta(\tau - \tau_0)$, which is not the case in $\alpha_0(t)$ due to the presence of f_c.

Let $H(t,f)$ be the frequency response of $h(t,\tau)$:

$$H(t,f) = \alpha_0(t)e^{-j2\pi f\tau_0}e^{j2\pi\Delta ft} \quad (6)$$

After transmission over this channel, the subcarrier n of the kth received OFDM symbol $y_{n,k}$ is given in the frequency domain (after removing cyclic prefix and taking DFT) by :

$$\mathbf{y}_k \;=\; \mathbf{H}_k\ \mathbf{s}_k + \mathbf{w}_k \quad (7)$$

where $\mathbf{s}_k = \left[s_{0,k},,...,s_{N-1,k}\right]^T$. Vectors $\mathbf{y}_k$ and $\mathbf{w}_k$ are defined in a similar way as $\mathbf{s}_k$. $\mathbf{w}_k$ is a white complex Gaussian noise vector of covariance matrix $\sigma_w^2\mathbf{I}_N$ and $\mathbf{H}_k$ is the $N \times N$ channel matrix. The entries of $\mathbf{H}_k$ are given by [5]:

$$[\mathbf{H}_k]_{n,m} = \frac{1}{N}\sum_{q=0}^{N-1} e^{j2\pi\frac{m-n}{N}q} H(kT_{\text{sym}} + qT_s, \frac{m - N/2}{NT_s}),$$
$$n = 0,\dots N-1,\ m = 0,\dots N-1 \quad (8)$$

Using (6), we get:

$$[\mathbf{H}_k]_{n,m} = \frac{1}{N}\sum_{q=0}^{N-1} e^{j2\pi\frac{m-n}{N}q}\alpha_0(kT_{\text{sym}} + qT_s)$$
$$\times\, e^{-j2\pi\frac{m-N/2}{NT_s}\tau_0} e^{j2\pi\Delta f(kT_{\text{sym}}+qT_s)} \quad (9)$$

B. Calculation of the ICI power

The power distributed on the nth subcarrier from the symbol $s_{m,k}$ on the mth subcarrier is:

$$\begin{aligned} P_{n,m} &= \left|[\mathbf{H}_k]_{n,m}s_{m,k}\right|^2 \\ &= \frac{1}{N^2}\sum_{q_1=0}^{N-1}\sum_{q_2=0}^{N-1}\alpha_0(kT_{\text{sym}} + q_1T_s)\alpha_0^*(kT_{\text{sym}} + q_2T_s) \\ &\quad \times e^{j2\pi\frac{m-n}{N}(q_1-q_2)} e^{j2\pi\Delta f(q_1-q_2)T_s} \\ &= \frac{\rho_0^2}{N^2}\sum_{q_1=0}^{N-1}\sum_{q_2=0}^{N-1} e^{j2\pi(q_1-q_2)\left(\frac{m-n}{N}+(\Delta f - f_D cos(\theta_0))T_s\right)} \\ &= P(m-n) \end{aligned} \quad (10)$$

Then, each null subcarrier receives a power of $P(-1)$ from the previous subcarrier and $P(1)$ from the next subcarrier, yielding an ICI power of $P(-1) + P(1)$. The theoretical power ratio to be compared with the measured one of section III is thus:

$$R = \frac{P(-1) + P(1)}{P(0)} \quad (11)$$

C. Comparison with the measurements

Using the frequency shifts observed in Section II-B, we compute the theoretical ICI power (11) as $R = -16.8$ dB for Run 3 and $R = -20.4$ dB for Run 1. Comparing these values with the ones obtained from the experiments it can be seen that they are 2-4dB lower than the measured ones. This is not very surprising, since (i) we have neglected other imperfections such as phase noise; and (ii) the channel model used in the theoretical calculations is a simplification of the reality. Nevertheless, the numbers are within the same order of magnitude, which lets us conclude that the theoretical model is a good approximation of the measured scenario.

V. Conclusions

This paper presented a study about the inter-carrier interference (ICI) that occurs in high mobility with OFDM modulations. We base our study on a high-speed train channel sounding measurement campaign carried out in the context of the project CORRIDOR. The ICI was measured both experimentally, by exploiting nulled out subcarriers in the sounding signal, and theoretically, by analytical computation using a simple channel model. We present results for the scenario where the train approaches the eNB, which results in a strong line-of-sight (LOS) with a deterministic Doppler shift. The analysis shows that the measurements match well the theory for this scenario.

Acknowledgments

This work has been supported by the project CORRIDOR (ANR).

References

[1] F. Kaltenberger and et al., "Broadband wireless channel measurements for high sp eed trains," in *ICC*, 2015.

[2] Z. Tang, R. C. Cannizzaro, G. Leus, and P. Banelli, "Pilot-assisted time-varying channel estimation for OFDM systems," *IEEE Trans. Signal Process.*, vol. 55, pp. 2226–2238, 2007.

[3] T. Zemen and C. F. Mecklenbrauker, "Time-variant channel estimation using discrete prolate spheroidal sequences," *IEEE Trans. Signal Process.*, vol. 53, no. 9, pp. 3597–3607, 2005.

[4] H. Hijazi and L. Ros, "Joint Data QR-Detection and Kalman Estimation for OFDM Time-varying Rayleigh Channel Complex Gains," *IEEE Trans. Comm.*, vol. 58, pp. 170–178, 2010.

[5] E. P. Simon, L. Ros, H. Hijazi, and M. Ghogho, "Joint Carrier Frequency Offset and Channel Estimation for OFDM Systems via the EM Algorithm in the Presence of Very High Mobility," *IEEE Trans. Signal Process.*, vol. 60, no. 2, pp. 754–765, Feb. 2012.

[6] E. P. Simon and M. A. Khalighi, "Iterative Soft-Kalman channel estimation for fast time-varying MIMO-OFDM channels," *IEEE Wirel. Commun. Lett.*, vol. 2, no. 6, pp. 599–602, 2013.

[7] HUBER+SUHNER, "Sencity rail excel antenna SPA-2400/50/12/10/V," Datasheet, Jun. 2012. [Online]. Available: http://goo.gl/xBHSv2